doi: 10.5028/jatm.v10.716

REVIEW ARTICLE

Low Subsonic Wind Tunnel – Design and Construction

Odenir de Almeida[1], Frederico Carnevalli de Miranda[1], Olivio Ferreira Neto[1], Fernanda Guimarães Saad[1]

Almeida O https://orcid.org/0000-0002-2204-1087
Miranda FC https://orcid.org/0000-0002-6648-4031
Ferreira Neto O https://0000-0003-1655-887X
Saad FG https://orcid.org/0000-0002-9357-1915

How to cite

Almeida O; Miranda FC; Ferreira Neto O; Saad FG (2018). Low Subsonic Wind Tunnel – Design and Construction. J Aerosp Tecnol Manag, 10: e1018. doi: 10.5028/jatm.v10.716.

ABSTRACT: This paper describes the design and the construction details of a medium size subsonic low-speed wind tunnel, which has been designed to achieve 90 m/s in the working section with expected low intensity turbulence level, making it available for researching in areas such as low speed aerodynamics (flight and terrestrial vehicles), sport activities, civil engineering applications, fundamental research in Fluid Mechanics and other possibilities. To accomplish such objectives a very detailed design was carried on using theoretical analyses, CFD simulations and semi-empirical methods, all of them applied to improve the flow quality along the wind tunnel sections. A very careful attention has been focused to the design of the fan blades and the electrical engine assembly, which has been inserted in a "pusher" configuration. Flow control and stabilization also took place using screens, honeycombs and corner vanes, all of them optimized to induce low turbulence levels in the working section. The design and construction of each wind tunnel section has been presented and discussed shedding light to the most relevant technical aspects and an attempt is made here to present some design and manufacture guidance for the main components of a low subsonic wind tunnel.

KEYWORDS: Wind tunnel, Low speed, Aerodynamics, Flow control, Turbulence.

INTRODUCTION

The practice of low-speed experimental aerodynamics has continued to evolve and it is a cornerstone in the development of a wide range of vehicles and other devices that must perform their functions in the face of forces imposed by strong flows of air or water. It was believed that in the 1970s and in the early 1980s the use of wind tunnels, especially in the subsonic regime, would rapidly disappear as computational fluid dynamics (CFD) would become a more attractive option to obtain data for many engineering applications, since it would be better in cost-effectiveness (Barlow *et al.* 1999). Nevertheless, computational simulations improved since then but they have not come close to reaching a level sufficient to replace the need for experimental data in development projects.

In fact, the investigative methods leading to quantitative predictions have been a combination of experiment and theory, with computational methods becoming a new powerful tool in this field. However, experimental explorations remain the mainstay for obtaining data to designers to achieve detailed results and final decisions across a broad range of industrial and academic applications. A primary tool for experimental aerodynamics is the wind tunnel. A well-designed wind tunnel

1.Universidade Federal de Uberlândia – Faculdade de Engenharia Mecânica – Centro de Pesquisa em Aerodinâmica Experimental – Uberlândia/MG – Brazil. **Correspondence author:** Odenir de Almeida | Universidade Federal de Uberlândia – Faculdade de Engenharia Mecânica – Centro de Pesquisa em Aerodinâmica Experimental | Avenida João Naves de Ávila, 2.121 – Santa Mônica | CEP: 38.400-902 – Uberlândia/MG – Brazil | Email: odenir.almeida@ufu.br

Received: June 10, 2016 | **Accepted:** May 18, 2017

Section Editor: Ana Cristina Avelar

could supply technical information for a large number of engineering applications such as external aerodynamics (flow over terrestrial and aerial vehicles), civil engineering (flow over bridges, buildings, cables, etc.), sport activities (flow over cyclists, design of volley and basket balls, wind sails etc.), fundamental fluid dynamics (laminar and turbulent flow over simple and complex geometries) and an extensive frame of other options in industry and research centers at universities around the world.

To achieve such level of applicability, there are 2 basic types of wind tunnels and 2 basic test section configurations, respectively. The 2 basic types of wind tunnels are open-circuit and closed-circuit. The advantages of open-circuit wind tunnels are the construction cost (less than closed-circuit), the possibility to run internal combustion engines and extensively use of smoke for flow visualization without the need to purge. The disadvantages are: harder than closed-test section circuit to obtain high-quality flow; wind and cold weather might affect operation; requires more energy to run if the tunnel has a high utilization rate; in general, it tends to be noisy. On the other hand, the advantages of closed-circuit wind tunnels are: using corner turning vanes and screens the quality of the flow can be well-controlled; independent of other activities in the building and weather conditions; less energy required for high utilization rates; less environmental noise when operating. The disadvantages are the higher initial costs (due to return ducts and corner turning vanes), the necessity to purge the tunnel if smoke is extensively used and some method of cooling for high utilization of the tunnel (Barlow *et al*. 1999; Mehta and Bradshaw 1979).

According to wind tunnel design, there are also 2 basic test section configurations which could be open-test section and closed-test section, which are respectively a free boundary test section (opened to atmospheric condition) and an enclosed test section (surrounded by walls), as illustrated in Fig. 1.

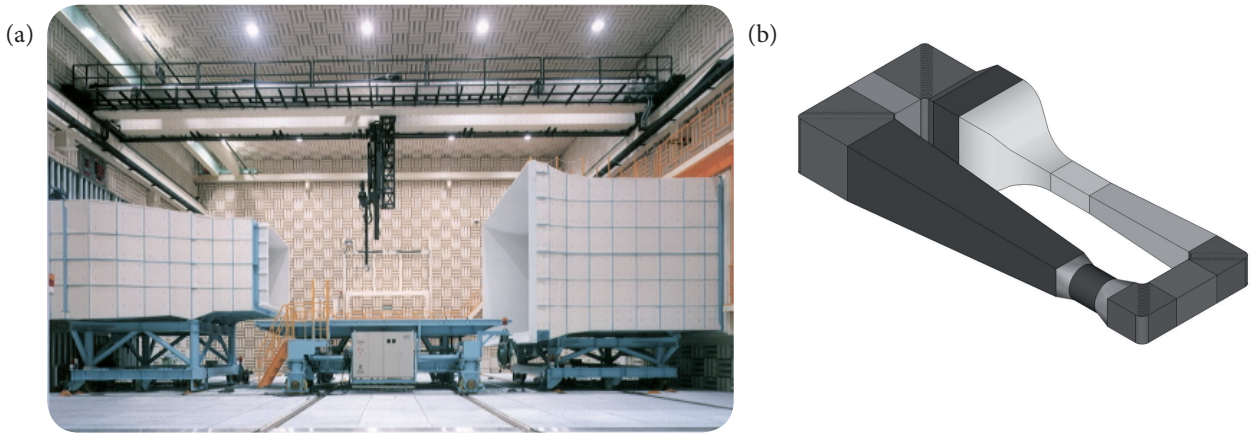

Figure 1. (a) Open test section (RTRI 2017); (b) Closed test section.

This paper aims to describe some aspects of the design and the construction details of a closed-circuit (closed-test section) subsonic low-speed wind tunnel, which has been designed to achieve 90 m/s in the working section with expected low turbulence intensity. To achieve such main goals a very detailed design was carried on through the use of theoretical analyses, CFD simulations and semi-empirical methods to improve the flow quality along the wind tunnel sections. A very careful attention has been focused in the design of the fan blades and the electrical engine assembly. Flow control and stabilization also took place using screens, honeycombs and corner vanes, all of them optimized for the best characteristics of the main flow. In addition to the design, special attention was taken during the fabrication process, not only including the right materials and construction techniques but also controlling the tolerances, gaps, steps and surface quality all over the wind tunnel sections. The main contribution of this study is to provide guidance by sharing experience for designing the wind tunnel components and parts, like test section, contraction, settling chamber and all the other sections, shedding light to the most important design parameters. Moreover, this technical research provides some construction ideas and tips that may apply to those ones interested to build such equipment. Based on these main

observations, the design and construction of each wind tunnel section has been presented and discussed based on these aspects, according to the following sections.

WIND TUNNEL DESIGN

Several references are known for wind tunnel design in open literature. However, special attention must be taken when considering aspects of low turbulence intensity, flow control and uniformity of the flow inside the wind tunnel as well as cost requirements, manufacturing process and future possible improvements in the equipment. According to these references, some traditional rules may apply with subtle corrections and/or adjustments for each specific design and application. The following main references have been consulted for designing the object of this study — a low-speed wind tunnel: Muncey and Pote (1956), Mehta and Bradshaw (1979), Barlow *et al.* (1999), Cattafesta *et al.* (2010), Bell and Mehta (1988, 1989), Lindgren and Johansson (2002), and Calautit *et al.* (2014). In the next sections, the wind tunnel design's requirements and the detailing of each component will be provided including the main technical aspects related.

WIND TUNNEL DESIGN REQUIREMENTS

The main requirements for this specific wind tunnel were defined at the beginning as: low-speed (subsonic at Mach 0.26) wind tunnel for research and educational purposes, closed-circuit/closed-test section with passive flow control (corner vanes and stabilization chamber). The design criteria have been set to enable accurate measurements of steady or unsteady flow with low turbulence intensity to facilitate the study of the physical phenomena of interest. Moreover, provisions were considered in the wind tunnel design for further boundary-layer transitions experiments and aeroacoustics analysis. According to these requirements, the main characteristics of the wind tunnel were defined as:

- Closed-circuit wind tunnel with approximately 30 m (length) and 10 m (width). The first drawings suggested a major section chamber of order 5 m × 5 m, for the contraction size.
- The wind tunnel material would be either naval-wood or steel plates for covering the sides of sections. Requirements for surface treatment have been considered like the polishing at surfaces and covering of any screw and/or slot present in each section. The whole structure (skeleton) could be either wood and/or metal bars as the construction of an aircraft's fuselage.
- The maximum air speed at test chamber must reach 90 m/s with a prescribed turbulence level around 0.2 – 0.5%.
- Minimum flow velocity: 5 m/s
- Test chamber dimensions: 1.7 m (width), 1.2 m (height), with 3.0 m (length).
- The test chamber must have access through acrylic doors.
- Inclusion of a stabilization chamber with screens and honeycombs for passive flow control.
- Contraction ratio between 9:1 and 12:1 to reach speed requirements.
- Minimum accessories: 2 Pitot tubes; fixed (used as reference) and movable, all of them connected with a digital pressure manometer.
- Drive System: electrical engine three-phase with 8 poles, 380 V and 350 hp equipped with an air or water cooling system, and fairing integrated to reduce flow disturbance and heating.
- Engine speed control: through frequency inverter.
- Fan blades: 8 blades of composite material, with approximately 3 m diameter and adjustable pitch for reaching optimum operational condition.
- The drive system must be structural isolated from other sections of the tunnel to avoid vibration.

Figure 2 shows a schematic view of the closed-circuit wind tunnel and its parts (sections). Some aspects of the wind tunnel design are described in the following sections.

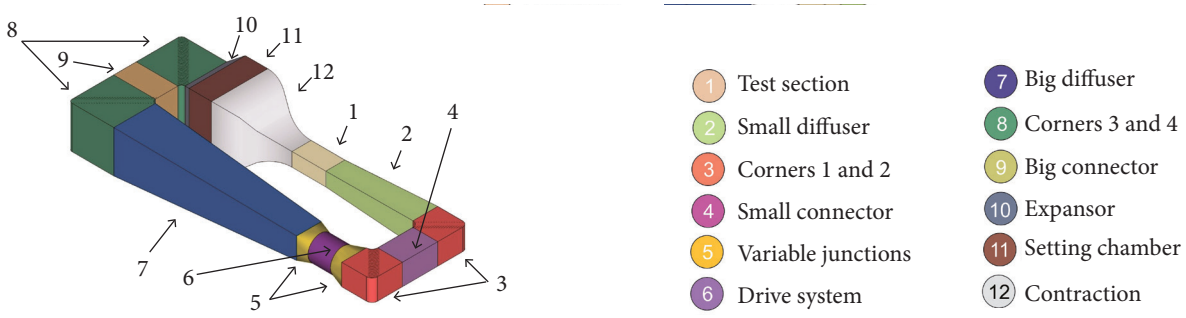

Figure 2. Closed-circuit wind tunnel — sketch and part description.

TEST SECTION

According to Barlow *et al.* (1999), the first step in the design of a wind tunnel is to determine the size and shape of the test section. This choice depends on the intended uses of the facility and, as will be discussed, is intrinsically linked to financial resources available to build the equipment. What we called scale factor was considered at the initial design stage, considering flight vehicles cruising below Mach number of 0.3 and with span close to 17 m, giving a scale factors in the range of 1:10 up to 1:20. The test section was originally designed with 1.70 m (width), 1.20 m (height) and 3.0 m (length). An approximation to the available Reynolds number in atmospheric conditions is in the range of 300,000 up to 7×10^5, providing satisfactory speed limits for the models that could be accommodated inside the closed-test section. Figure 3 illustrates the geometric sizing of the test section. It was constructed according to the requirements; including a large access door made of acrylic for making easy the application of visualization techniques such as smoke's rake or particle image velocimetry (PIV). The other lateral panels could be replaced at any time with acrylic panels and/or other specific material such as laminated wood. The test section illumination was completed with light emitting diode (LED) lamps over the floor and ceiling along its length. At the floor, there was the access platform to the aerodynamics balance, which is a circular disk of 1 m in diameter. A common rule of thumb has been set in accordance with Mehta and Bradshaw (1979), were the test section rectangular dimension sizing is around 1.4:1. The results for the boundary layer estimates in the test section will be shown in the CFD analysis section.

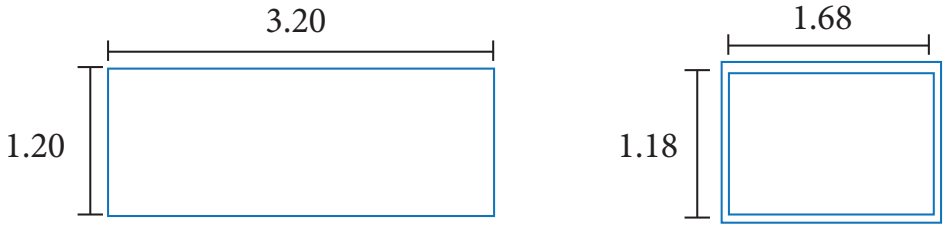

Figure 3. Geometric sizing of the closed test section.

DIFFUSERS

The diffuser of a closed-circuit wind tunnel extends from the downstream end of test section (small diffuser, according to Fig. 2) to the third corner of the tunnel, being divided in 2 parts by the tunnel fan (Barlow *et al.* 1999). The second diffuser (big diffuser as seen in Fig. 2) is often named the return duct since it directs the flows towards the test section. Since the power losses at any point in the tunnel are expected to vary as the speed cubed, the main purpose of the diffuser is to reduce the speed with as little energy loss as possible which means maximum pressure recovery, reducing the load of the drive system. Also, the pattern of the flow leaving the test section influences the flow field inside the diffuser. The

flow properties like orientation, size and wake development from models affect the diffuser entrance flow. The primary design parameters for a diffuser are the equivalent conical expansion angle and the area ratio (Barlow *et al.* 1999).

The small diffuser was designed with an inlet area (A_i) of 1.2 × 1.7 m² and having an exit area (A_e) of 1.85 × 1.85 m² with a length of 8.0 m (Fig. 4a). The expansion ratio (A_e/A_i) is 2.00, being the ratio between the diffusor's length (L_D) and the entrance height (H_i) approximately 6.65. The small diffuser half angle's value is 2.5. At the end of this diffuser was installed a safety screen to avoid any loose parts from the test section to be carried to the drive system. The second diffuser is installed after the drive system and has 15 m length with exit dimensions of 3.7 × 3.7 m². The expansion ratio (A_e/A_i) is 2.10, being the ratio between L_D and H_i around 8.11. The big diffuser half angle's value is also 2.5. A second safety screen was placed at the end of this diffuser to retain any part lost from the drive system assembly. The diffuser expansion factor must be well evaluated to avoid flow detachment (Mehta and Bradshaw 1979). Knowing this, the area of the diffuser should increase gradually along its axis to avoid flow separation and its geometry can be optimized. Kline's flat diffuser curves (Runstadler *et al.* 1975) are often used for diffuser's design (Fig. 4b).

The area ratio (*AR*) between the diffuser's exit and entrance is plotted *versus* the ratio of diffuser length to the entrance height of the diffuser. Three regions are shown on the plot in Fig. 4b, the design of the diffuser is conducted by selecting a length for the diffuser, that is, within facility size constraints. Given L_D/H_i (where the height is dictated by the test section size), the corresponding value of *AR* is selected from the no-stall regions. Although a greater pressure recovery can be achieved by operating in the "unsteady flow" regime, this can contribute to unwanted noise, as well as poor performance at off-design flow conditions. If facility constraints limit the length of the diffuser or a closed-circuit design is used, a turning section with guide vanes can be used, and the diffuser can be broken into multiple sections. In Fig. 4b, it is shown the design point (in red) for both diffusers defined in this study.

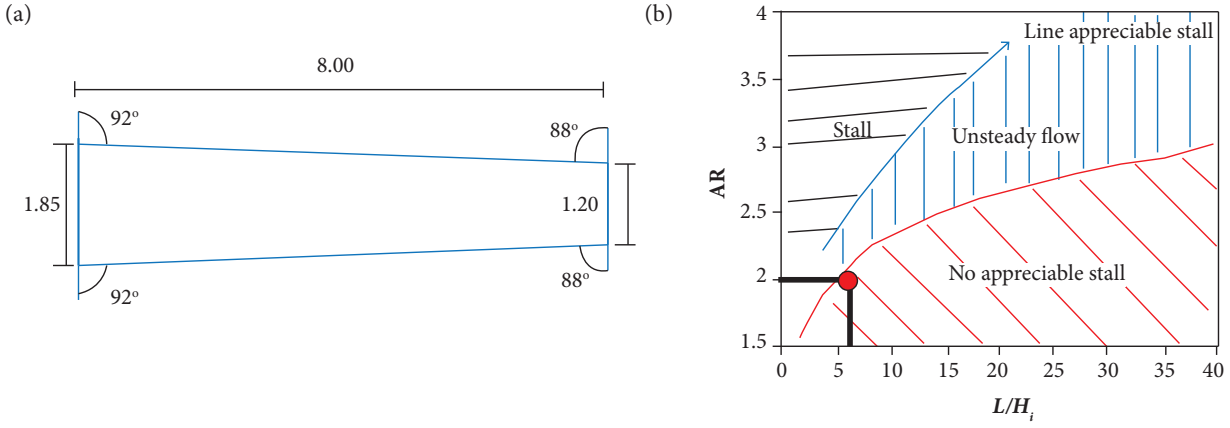

Figure 4. (a) Geometric sizing (small diffuser); (b) Diffuser design curves. Adapted from Runstadler *et al.* (1975).

CORNERS 1, 2, 3 AND 4

The corners of a closed-circuit wind tunnel require special attention since they have the important task to turn the flow by 90° and to keep it organized, *e.g.* without regions of separation and recirculation. To accomplish such task 2 sets of corners have been designed and built, corners 1 and 2 after the small diffuser and corners 3 and 4 just after the big diffuser. The corners 1 and 2 have dimensions of 1.85 × 1.85 m² in the entry and exit areas. The corners placed after the long diffuser have dimensions of 3.7 × 3.7 m² in the entry and exit areas (Fig. 5a and 5b).

As seen in Fig. 5, both set of corners were integrated with turning or corners vanes specially designed to turn the flow by 90° at the bend. Also, these turning vanes are quite important to avoid large losses and to maintain relatively straight flow inside the channel. According to Barlow *et al.* (1999), it is usual to keep the corners with constant area. It is possible to reduce the losses in the turning vanes by selecting an efficient cross-sectional shape and by using an appropriate chord-to-gap ratio. The shape of the

corner vane has been based on Lindgren and Johansson (2002), Fig. 6, with an increase in the thickness of the airfoil. The set of points that describe the geometry of the corner used is listed in Table 1.

In this study, the small corners have 7 turning-vanes while the big corners have 12 to keep the ratio of the gap to the chord (h/c) about 0.25. This is an important parameter to reduce the losses at the corners, as described in Barlow *et al.* (1999) and Lindgren and Johansson (2002).

The final configuration of the wind tunnel will incorporate corner vanes that are screwed with adjustable pitch, which means that any eventual flow correction may also apply by turning the vanes inside the corner, thus improving the flow quality and reducing the losses at the bends of the wind tunnel.

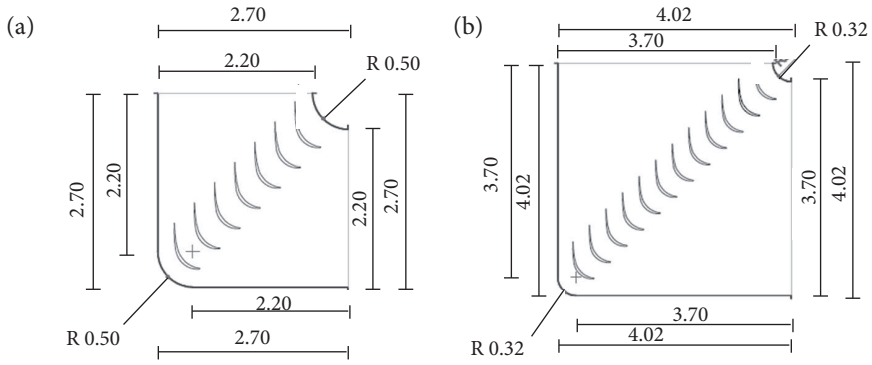

Figure 5. Geometric sizing of corners. (a) Corners 1 and 2; (b) Corners 3 and 4.

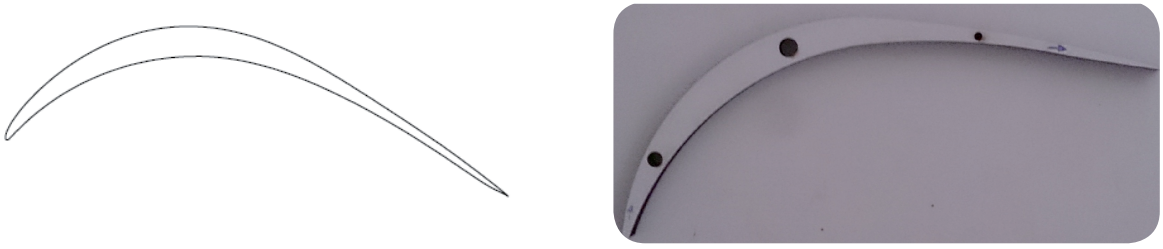

Figure 6. Design of the corner vane based on Lindgren and Johansson (2002).

Table 1. Corner vane points.

X	Y	X	Y
0.00	0.00	0.36	1.00
0.00	0.06	0.46	0.97
0.01	0.12	0.54	0.88
0.02	0.21	0.65	0.68
0.07	0.44	0.72	0.49
0.16	0.75	0.85	0.14
0.23	0.88	0.90	0.00
		1.00	−0.30

DRIVE SYSTEM

The drive system determines how the working fluid is moved through the test section, being its selection dependent on the medium and the operational regime for the wind tunnel. Fans tend to work best with low-speed facilities and are rated by the volume flow rate and the static pressure drop they can overcome. This component generates a volume flow rate and compensates

the remaining pressure losses. Barlow *et al.* (1999) provide a procedure for estimating the losses incurred in the closed-circuit tunnel, helping in the fan selection. To keep a flow velocity of 90 m/s at the test section the drive system is composed by an electrical engine with 350 hp equipped with an air cooling system. The axial fan efficiency is 0.90, and the global charge losses factor is 0.50. Other parameters like friction loss 0.07; losses on screen hives and drivers 0.18 and loss on diffusor 0.25 were considered to estimate the global charge losses factor. Since the test section area is 2.040 m^2, the described drive system will assure a mass flow of 170.311 kg/s, a volume flow of 151.522 m^3/s and a dynamic pressure of 3100 Pa. The engine is assembled with 8 fan blades with approximately 1 m long (Fig. 7). An engine cowling was designed completely streamlined with the flow using fairings for covering the engine chassis (Fig. 7). The air cooling system is forced by use of 2 additional small centrifugal blowers through ducts inside the main fairing. The engine has been assembly in a "pusher" configuration as a design choice. With this engine configuration and the design of efficient blades, it is expected an addition of energy to the main flow that could increase the speed values in the test section. As seen in Fig. 7, the whole engine assembly was kept "clean" and reduced in size. To reduce the blade's swirl a set of stator-vanes (not shown in Fig. 7) will help to rightly direct the flow inside the channel towards the big diffuser. The impact of the engine assembly in the flow uniformity and pressure losses could be further evaluated through empirical tests with the wind tunnel in operation.

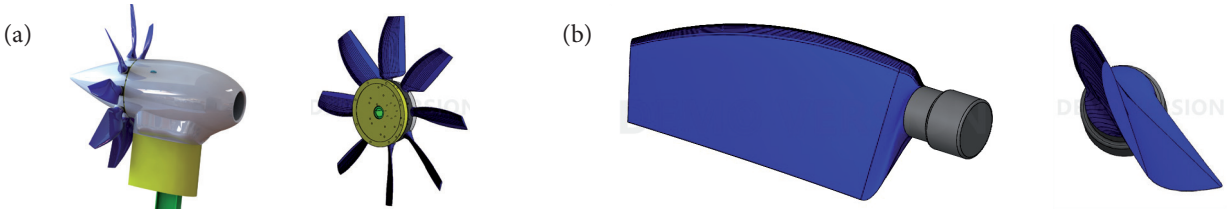

Figure 7. (a) Engine assembly; (b) Blade design.

For the blades design, the Blade Element Theory (Lan and Roskam 1997; Pawlowski 1920) was applied with the following parameters considered: number of blades (8), motor speed (890 rpm), propeller diameter (2.2 m), spinner diameter (0.8 m), maximum operational speed at pumping chamber (48.3 m/s), maximum available power supplied by the electrical motor (260 kW); and atmospheric parameters: air density [ρ = 1.06428 kg/m^3 at 884 m, International Standard Atmosphere (ISA) + ΔT = 16 °C], kinematic viscosity (ν = 1.657e-5m^2/s) and speed of sound (a = 346.28 m/s). The complete description of the blade's design could be found in Almeida *et al.* (2016).

The whole drive system was completely segregated from the wind tunnel, *i.e.* there is no hard and/or physical connection between the engine and the wind tunnel structure (Fig. 8). With the engine support and the drive system's chamber isolated, it is expected low vibration in the structure and less impact in the flow uniformity. Also, to avoid pulsations of the flow inside the chambers, a slot (about 0.1 m^2 of diameter) or so called "breather" was inserted in the small diffuser. This slot was covered with a fine screen to prevent any external light material from entering the tunnel.

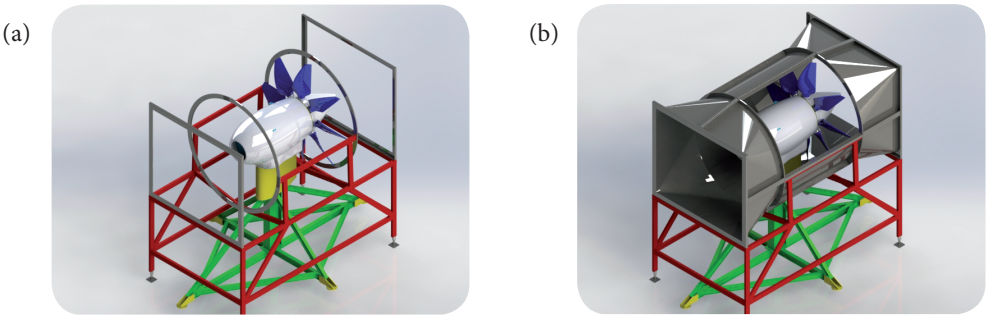

Figure 8. (a) Description of the engine support; (b) Drive system chamber.

CONTRACTION

The contraction has a great importance in determining the flow quality in the test section. According to Derbunivich *et al.* (1987), the contraction accelerates and aligns the flow into the test section. In addition to these benefits, the contraction section is responsible to stretch vortex filaments, which reduces axial but intensifies lateral turbulent fluctuations, as discussed by Tennekes and Lumley (1972). The length of the contraction should be sufficiently small to minimize boundary-layer growth and production cost but, long enough, to prevent large adverse pressure gradients along the wall, originated by streamline curvature, this phenomenon can lead to flow separation. Morel (1975) suggested a simple analytical method of matched polynomials, as shown in Fig. 9.

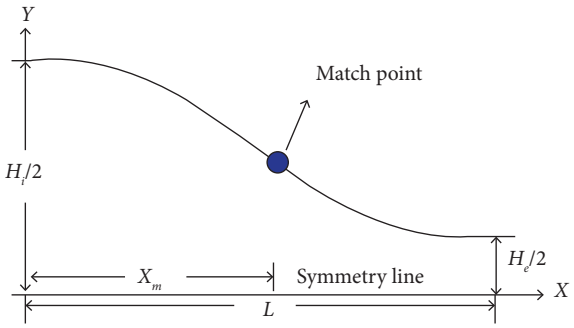

Figure 9. Schematics of the contraction shape with matched polynomials after Morel (1975).

In Fig. 9 the entrance height of the contraction is H_i, and the exit height is H_e. The total length of the contraction is L_C, and the 2 polynomials are matched (location, slope, and curvature) at a specified location $x = x_m$. At the exit of the contraction, any remaining "free" higher-order derivatives of the polynomial are set to 0 to obtain a straight section. Another way was recommended by Su (1991), which consists on matching a cubic polynomial at the contraction entrance with a higher-order polynomial at the contraction exit. Contractions with minimal flow nonuniformities can be designed by iteratively selecting the entrance height, contraction ratio, match point, and length of the contraction. Techniques using 3-D potential flow simulations inside the contraction followed by the application of Stratford's (1959) separation criteria for turbulent boundary layers affected by adverse pressure gradients could also be applied to develop optimized contractions meeting design criteria for test section flow uniformity (Mathew 2005).

In this paper, the contraction was designed according to Morel (1975) and following Su (1991) providing a contraction ratio of 12:1 to meet the velocity requirements inside the test section. According to Mehta and Bradshaw (1979), the design of a contraction is aimed to reach a uniform and steady flow at its outlet, and requires the avoidance of flow separation. Based on these rules, it has been selected a tradeoff between contraction length and contraction ratio, since as a design choice it has been invested in the insertion of a settling chamber (including honeycombs and screens) before the contraction. In this case, it is expected that a higher contraction ratio could take place without jeopardizing the flow uniformity in the test section. Figure 10 shows the contraction curve designed to reach a 1st and 2nd derivative at the inlet and outlet. Also, the selected curve was applied to a tridimensional CFD model to verify the development of the boundary layer inside the test section. These results will be revealed in the computational part of this study.

SETTLING CHAMBER

Despite the difficulties imposed by the large size of the contraction (5m × 5m), a set of honeycombs and screens has been incorporated in the design of the settling chamber. This section is also depicted in Fig. 10 and has dimension of 5m × 5m (cross-sectional area) and 2 m (length). Before entering into the settling chamber there is a large screen after the corner 4 with 2 main objectives: to stop any part lost from the drive system and to add uniformity into the flow, breaking the large-scale structures which may be present in the incoming stream. Thus, between the expansion from corner 4 and the contraction was placed the settling chamber with a set of an aluminum honeycomb and screens. The design and sizing of cell to the screens and honeycomb have been carried out to reduce swirl and lateral mean velocity variations with a certain pressure drop. Some design tips and

recommendations were taken from Farell and Youssef (1992) and Barlow *et al.* (1999). The loss imposed by the honeycombs panels were below 5% of the total losses inside the wind tunnel. The constructive details are length (L_{SC}) = 48"; width (W_{SC}) = 96" and thickness (T_{SC}) = 4", with hexagonal cells of ½" made of aluminum (Fig. 11a). Due to the size of the contraction, it was necessary to include 10 panels to cover all extension of 5 m × 5 m for the square section at that position (Fig. 11b).

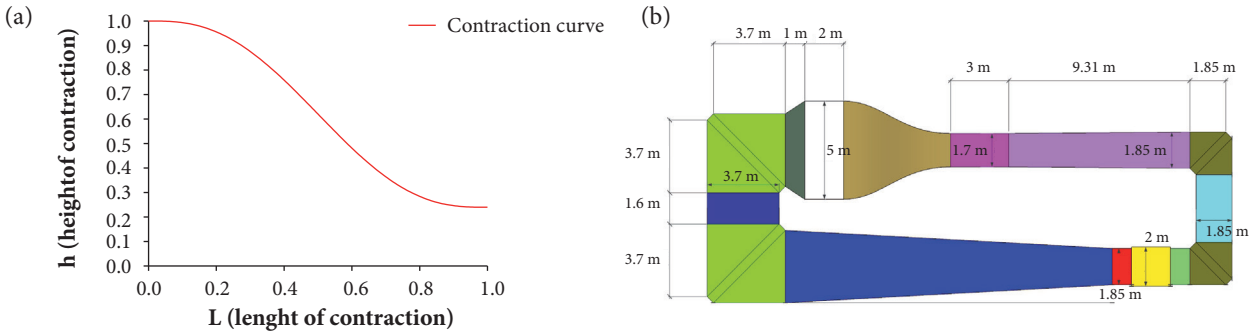

Figure 10. (a) Contraction curve; (b) Geometric sizing.

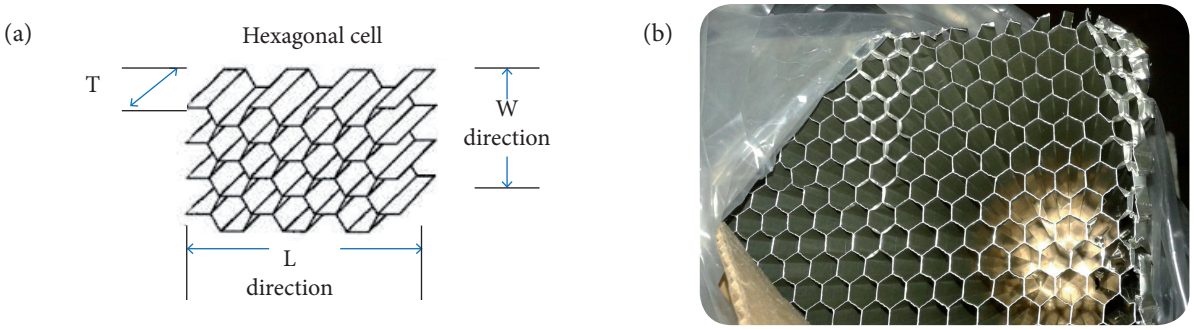

Figure 11. (a) Honeycomb sizing; (b) Honeycomb panel inserted in the settling chamber.

COMPUTATIONAL ANALYSES

The commercial ANSYS Fluent® numerical code was used for predicting the flow characteristics inside the closed-loop subsonic wind tunnel. All the computational analyses were performed by means of solving the Reynolds Averaged Navier-Stokes equations (RANS simulation) through a control-volume-based technique. The standard k-ε turbulence model was used for defining the turbulence kinetic energy and dissipation rate and a 2nd-order upwind scheme was used to discretize all the transport equations. Standard wall functions were used on the walls and the roughness constant was set to 0.5. The numerical code used the semi-implicit method for pressure-linked equations (SIMPLE) algorithm for the velocity-pressure coupling of the computation.

An initial simulation (conventional approach) was considered by taking a reduced size domain, including the contraction, the test section and the small diffuser. To achieve the maximum expected velocity (90 m/s) in the test section some trials have been performed to adjust the boundary condition at the inlet of the domain (inlet BC). Figure 12 illustrates the computational domain used in these simulations.

The simulations were run for 2 different flow velocities in the test section: (a) 12 m/s and (b) 85 m/s. All simulations were performed with a standard k-ε turbulence model and the convergence criterion was achieved with 4 orders of drop magnitude. Some snapshots of the flow inside the contraction and in the test section are presented in Fig. 13. The flow is well-organized through these wind tunnel sections. No large regions of flow's detachments were seen in the contraction allowing good flow uniformity

in the test section. Figure 13b represents the contours of velocity magnitude in a cross-sectional plane in the middle of the test section, were it is possible to see the development of the boundary layer. To estimate the boundary layer thickness this plot was taken over 2 positions, at the distances (L_b) of 1 m and at 3 m in the test sections, considering 2 different flow velocities in the test section: 12 and 85 m/s. The values are given in Table 2, where Ɛ represents the boundary layer thickness.

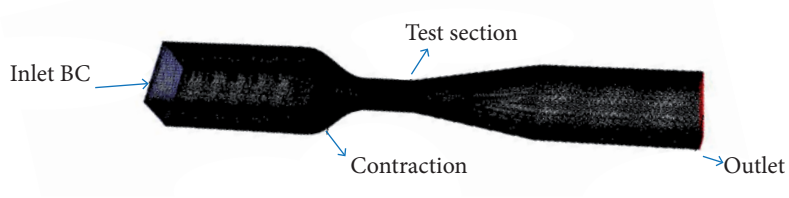

Figure 12. Reduced-size CFD computational domain for boundary layer estimation (conventional approach).

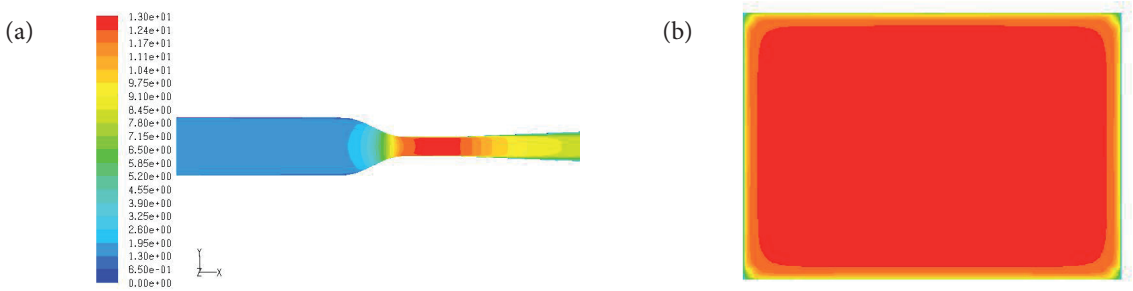

Figure 13. Contours of velocity magnitude. (a) Flow inside test-section; (b) Cross-sectional plane at mid-test- section.

Table 2. Boundary layer thickness obtained by CFD.

V	L_b (m)	Ɛ (m)
85 m/s	1.000	0.020
	3.000	0.052
12 m/s	1.000	0.030
	3.000	0.067

These CFD data have been corroborated by the analytical solution of the Blasius equations (White 2003). Figure 14 illustrates this comparison with a satisfactory match between the results.

Additionally, 2- and 3-D computational analyses of the whole wind tunnel were carried out during the development of this paper. Two sets of simplified 2-D simulations were conducted with and without corner vanes only to identify the main characteristics of the flow inside the channels. These results will not be presented here, for brevity purposes but, as expected, the results indicated a well-organized flow when the turning vanes were included in the simulations. As suggested by Moonen *et al.* (2006), a full-scale CFD model of the entire wind tunnel was considered instead of the conventional approach, in which only the flow in the test section was modeled. The established CFD method accounted for the influence of the corner vanes. This allowed for the understanding of the flow pattern not only in the test section but also the flow in other wind tunnel sections. The rationale behind choosing the k-epsilon model was the findings of previous study from Calautit *et al.* (2014), which showed its capabilities in predicting the wind tunnel flows. Air temperature of 25 °C (298.15 K) was applied as inlet boundary condition to the flow and the velocity-inlet set as 35 m/s. The outlet of the tunnel was set as pressure-outlet with 0-gauge pressure. The 3-D model of the wind tunnel with corner vanes is shown in Fig. 15, including the boundary conditions, and the complete mesh can be visualized in Fig. 16.

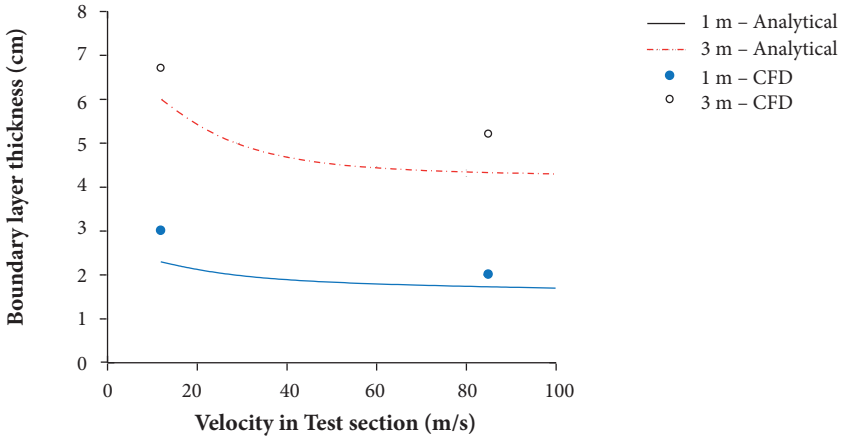

Figure 14. Comparison of boundary layer development (CFD *versus* analytical solution).

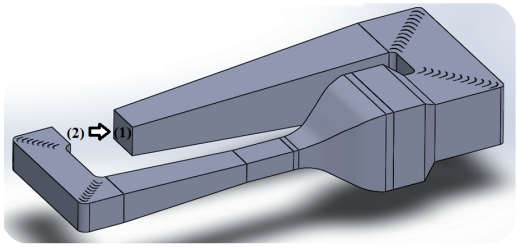

Figure 15. 3-D CAD model with corner vanes. (1) Velocity inlet; (2) Pressure outlet.

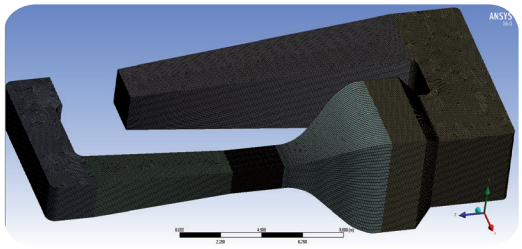

Figure 16. Mesh for the 3-D tunnel without corner vanes.

The velocity contours from the 3-D simulations for the wind tunnel without corner vanes and with corner vanes installed on it could be visualized in Figs. 17 and 18, respectively. By analyzing and comparing the results, it is possible to verify flow separations in the upstream and downstream side of the wind tunnel corners in the configuration without corner vanes (Fig. 18). The flow inside the settling chamber was also affected and it was not uniform as it should be in real conditions. On the opposite, with the insertion of the corner vanes the flow was more organized not only in both corners 3 and 4 but also in the settling chamber section. A detailed analysis of the flow quality inside the test section could be checked by inspecting the transversal (Y-height) and (X-width) velocity profiles.

The velocity profiles obtained from the 3-D simulations of the wind tunnel with and without corner vanes are shown in Figs. 19 and 20, respectively, for x (width) and y (height). By comparing the velocity profiles, it is possible to observe that the corner vanes made a very small difference on the flow quality at the test section, despite that, its influence was not good, making the flow without corner vanes better than with the vanes installed on the wind tunnel. The next profile (Fig. 20) is the height profile at test section (y direction). The same observation could be applied in this case as well.

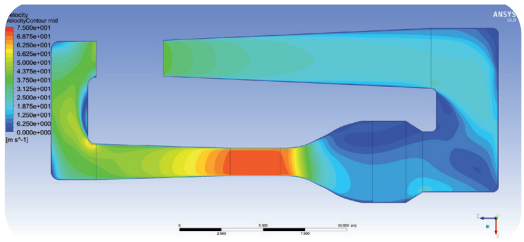

Figure 17. Velocity contours for the 3-D wind tunnel without corner vanes.

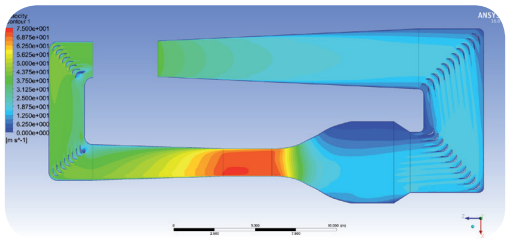

Figure 18. Velocity contours for the 3-D wind tunnel with corner vanes.

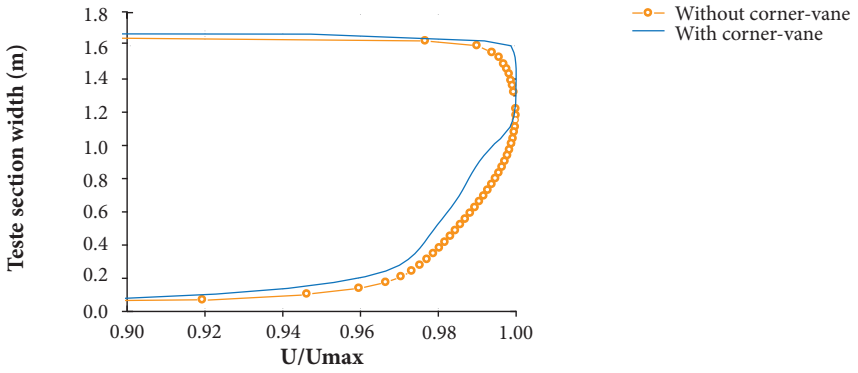

Figure 19. Velocity profile of the flow at the test section (width).

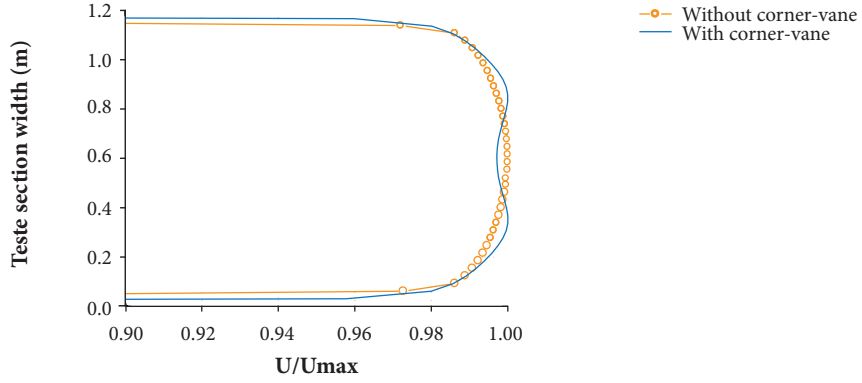

Figure 20. Velocity profile of the flow at the test section (height).

Actually, this result was not expected but, after a close look on the results and analyses of these profiles, we concluded that corner vanes have a strong effect in turning the flow 90° with a good pattern of organization; however, as identified in other studies, such as Lindgren and Johansson (2002), the vanes could be adjusted to have at least 5° of attack angle. In the simulations performed here, the attack angle was 0°, since the corner vanes were aligned by taking the trailing edge as reference. By considering this adjustment, we believe that the small regions of detached flow between corners 3 and 4 could be completely eliminated, reducing consequently the flow detachment in the settling chamber (Fig. 18). This recirculating flow in the settling chamber for the case with corner vane is impacting the flow uniformity in the test section, whose consequences are clearly seen in the velocity profiles of Figs. 19 and 20.

These computational analyses were performed to provide a general description of the flow inside the wind tunnel. Additional analyses were conducted during the development phase of the wind tunnel. Another important observation is that the settling chamber details (honeycombs and screens) were not included in these simulations and that is the reason of a high degree of non-uniformity in this wind tunnel section, as seen in the velocity contours, since the flow is separating just at the entry of this section. In the real situation, this is not expected to happen, since the screens and honeycombs will correct the flow right after.

WIND TUNNEL CONSTRUCTION

This section describes some details about the construction of this specific wind tunnel. As a design's decision, the wind tunnel parts were chosen to be like an aircraft fuselage. The structure has main spars and ribs made of steel and covered by a skin of naval wood, treated for humidity and having a high level of surface finishing, by employing an 18-mm medium density fiberboard (MDF) for the panels to cover the sides of sections. The welding method adopted was the metal inert gas (MIG) with 2 mm width. Figure 21 illustrates an example of one of the wind tunnel sections (smaller diffuser) designed according to this procedure. By using this type of structure, it is expected a long durability for the equipment also helping in other issues such vibration, regularity of internal surfaces, refurbishment of some specific parts among other aspects.

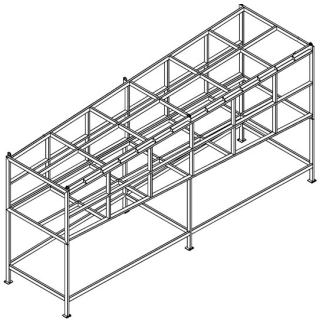

Figure 21. Wind tunnel construction like an aircraft's fuselage — smaller diffuser.

During the process of construction, the smaller diffuser (Fig. 22a) was the first part built, considering its simplicity. The small steel connection parts were cut by water-jet, allowing a great precision and delivering a good quality to the wind tunnel. The material used for all the structural parts of the tunnel, including the referred one, was the SAE1020 Steel with bars of 50 × 100 mm. The junction between wood panels has been sealed with plastic resign to avoid gaps and steps. In Fig. 22b, it is possible to see the high quality of the internal surface. This procedure has been extended for the construction of all other sections of the tunnel.

The test section was the second part constructed, and a special attention was given to fix the MDF's panel on the main structure by using polyvinyl chloride (PVC) glue that has a rubber base. By making this procedure, the vibration transferred to the wood panel was reduced, contributing to keep the flow laminar. In addition, each wood panel was screwed in the spars and ribs throughout the whole section. Internally, each screw was covered with plastic resign to meet the surface finishing requirements. To avoid slots

at the upper and lower corners (connection between the side wall panels) in all the connections it was used a composite based on PVC to seal the tunnel. As requirement, the test section has a polycarbonate door (transparent) hinged on three points and automatically actuated by an electric motor. An additional simple door was placed at the end of the test section to make easy the access into this chamber every time is needed. Figure 23 shows some details of the test section construction.

(a)  (b) 

Figure 22. (a) Smaller diffuser; (b) Internal finishing details.

 

Figure 23. Test section details.

The most complex part to be built was the contraction. Since the contraction curves assume a prescribed curvature function, the placing of the Naval MDF's took around 4 weeks. Bending the wood panels without distortions require time, caution and work skill of a good carpenter. The contraction part is shown in Fig. 24.

  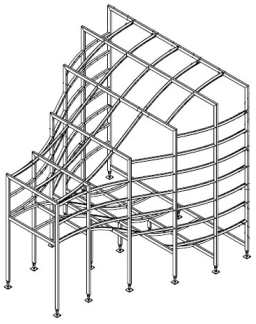

Figure 24. Contraction section (details of construction).

Other sections that deserved especial attention were the corners; they were built as one piece connected by the middle part between them (connectors), 2 parts in total (C1, C2, C3 and C4 connections). A correct design of this part is quite important to

impose a better flow control for bending it at 90°. It was possible to achieve a better strength and dimensional control with metal structure and wood panel. As cited before, it was used additional flow control by using corner turning vanes placed rightly to direct the flow. The material of the turning vanes is mainly fiberglass, to have good surface finishing and light weight. Sets of turning vanes were placed at both small corners (just after the section test) and at the big corners (after the long diffuser).

The corners C3 and C4 (after the big diffuser) and the profile of the turning vanes are shown in Fig. 25. The corner vanes are depicted in Fig. 26 inserted in the corner C1. Each corner vane could be adjusted manually, by moving them around the main axis to achieve different attack angles to better control the flow at the bend. As mentioned before, this wind tunnel section is quite important to the flow uniformity in the test section.

(a)  (b) 

Figure 25. (a) Corners C3 and C4 without the turning vanes; (b) Turning vane profile.

Figure 26. Turning-vanes mounted in the corner C1.

The drive system was the main concern during the design phase and later in the construction process, since it is the "heart" of the wind tunnel. According to the required power, the electrical engine weighted around 2 tons (2,000 kg) and required special attention to install it. To avoid large vibration transmission through the tunnel, when starting the engine and at higher velocities of operation, the engine was completely segregated by using a pyramidal support. For helping the flow quality across the pumping chamber, an aerodynamic fairing to the electrical engine was conceived, which associated to the pusher configuration, could help to increase the velocity inside the test section. Additionally, to remove the swirl from the blades in operation, stator-vanes were included just in front of the propeller disk. Figures 27a, 27b and 27c show the pyramidal support with the electric motor installed on it, the drive system section, and the cowling for the engine, respectively. In this figure, it is possible to see the engine intake that will get some amount of air from the main flow to cool down the engine. Also, to keep the air temperature inside the wind tunnel constant during all operational velocities, a cooling system is coupled with the engine nacelle which removes heated air inside the engine cavity due to the electrical dissipation and due to the close-circuit energy buildup. An additional 4 hp electrical engine is used to suck the air and to threw it away to the environment (Fig. 28).

The drive system also comprises a hub with 8 fan blades made of composite material (fiberglass) for propelling the air. This set of blades is pitch adjustable by means of mechanical action in the hub. The hub itself can be screwed off delivering rotational motion for each blade that could be adjusted by using a tool to correct the attack angle. Figure 29 shows a sketch of this hub configuration.

The adjustment of the pitch allows the engine to operate at safely margins minimizing the operational and maintenance costs during work life of this wind tunnel. The drive system is completely accessible via a maintenance door and the engine could be rapidly removed from this section if necessary. As mentioned in the design section, the blades were designed through the Blade Element Theory for achieving efficiency of order 90% throughout the operational envelope of this wind tunnel (Almeida *et al.* 2016).

(a) (b) (c)

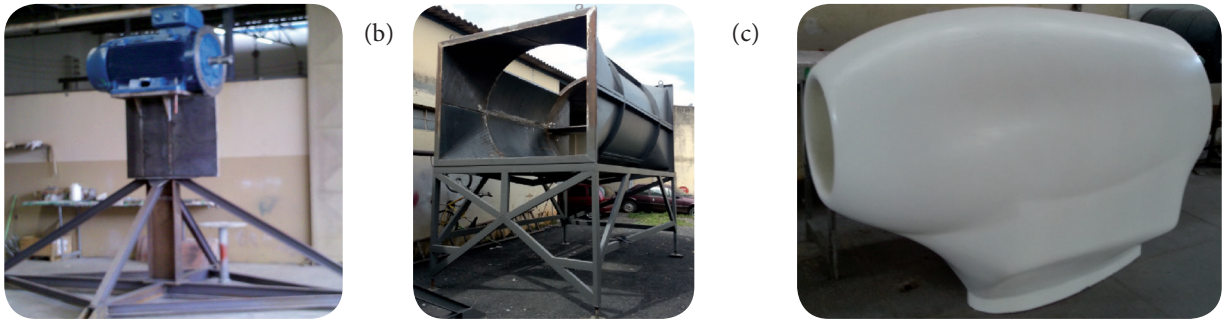

Figure 27. (a) Engine support; (b) Drive system section; (c) Engine fairing.

Figure 28. Cooling system to extract hot air inside the engine cavity.

(a) (b)

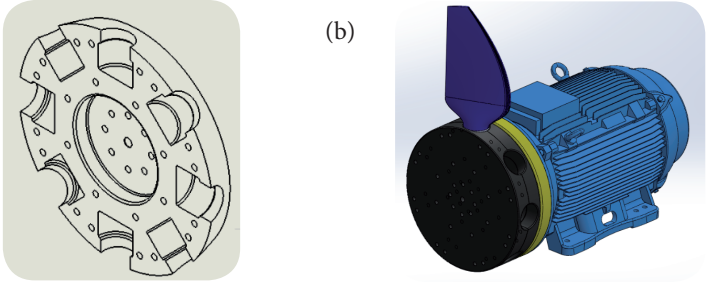

Figure 29. Blades pitch adjustable in the hub, (a) Part of the main hub; (b) Main hub assembly.

The blade manufacturing process was kept simple and efficient by using fiberglass lamination. The lower surface lamination was made separately from the upper surface, so that each of these processes required a different mold. Five layers of fiber glass and blanket were employed, each of these layers with lengths ranging from 100% of the form length, decreasing 10% to reach 60% of its total size. When the upper and lower surfaces were rolled, twisted yarns and small wood components were applied to improve the blade's structure. The whole set was then glued and assembled with screws fixing the forms for the drying process (Fig. 30). After this stage, the forms were detached so that the process of finishing and painting of the blades was performed, completing its manufacture. Figures 31 and 32 show the 8 finished blades of composite material and the view of the blades assembled in the engine, respectively.

(a) 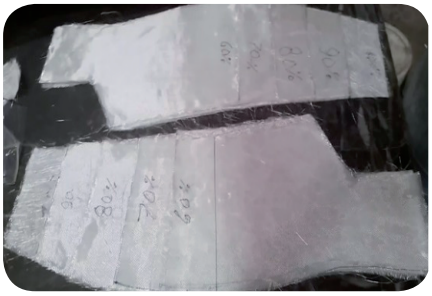 (b) 

Figure 30. (a) Fiberglass and blanket for blades manufacturing; (b) Lamination process in form.

(a)  (b) 

Figure 31. (a) Finished blade; (b) Blades set.

(a) 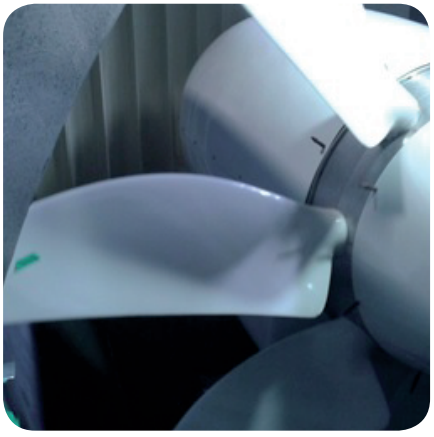 (b) 

Figure 32. (a) Blades-engine set front view; (b) Blades-engine set back view.

Finally, it is important to emphasize that all the structure steel parts of the tunnel were coated with anti-corrosion paint to have a higher durability. The wood panels were cleaned off and sealed after the construction. No "bumps" and/or surface deviation were allowable for the whole wind tunnel sections. Figure 33 illustrates the final wind tunnel completely assembled and ready for the initial tests and qualification. The whole wind tunnel construction took around 12 months with all parts being under quality inspection weekly. Any deviations from tolerances where adjusted during the fabrication process and/or even rebuild to achieve the requirements.

Figure 33. Panoramic view of the wind tunnel.

CONCLUDING REMARKS

The design and construction details of a closed-circuit, closed test section, low subsonic wind tunnel was presented. Analytical models were considered to describe the pressure losses and CFD was also applied to verify the quality of the flow inside the channels. The main conclusions and remarks are summarized as described in sequence, shedding light to the most important design parameters and observations gathered during this specific study:

- The wind tunnel design is somewhat not standard procedure and depends very strongly on variables such as infrastructure (space dimensions), flow speed requirements and mainly cost for production. The first 2 variables are quite sensitive to the need of educational and research purposes and can be dealt with rationale through the phases of design. The last variable (cost) imposes hard limitations to the design.
- The cost of the whole equipment and specific parts such as drive system can really push back the design for simpler configurations. Based on that, one of the most important phases of the design is not technical but economical. A complete "part-and-cost" list must be specified at the beginning of the design to provide estimates. A detailed specification must be followed by establishing contacts and invoice calls, thus refining the estimates and providing more realistic cost reference for the whole wind tunnel conception.
- The selection of turning-vanes is quite important to improve the flow quality in the test section. What is striking is to verify the impact of changing the angle of the flow. Based on this design experience, we recommend a set of different CFD simulations to check different airfoil designs and positioning. Otherwise, the inclusion of an adjustable mechanism to rightly orient the vanes could help significantly in the actual operational conditions.
- The drive system configuration is far the most complex point in the whole design. The choice for a segregated engine's support was clearly an excellent design option. During the first trials, there was not identified vibration in the whole equipment, even in the pumping chamber. The engine assembly is another point that deserves very careful attention, since it could impact the global losses for the whole tunnel. We have decided for the "pusher" configuration instead of conventional tractor. As mentioned, the first trials were promising and ensured good flow quality.
- The fan blade, as well as the turning vanes design, is clearly very important to the wind tunnel performance. The design of airfoils and propelling blades has received a large amount of attention in the last decades and is given now to the designer some satisfactory tools for designing such devices. We recommend tests with different methodologies before deciding which one could be used to provide the final airfoil/blade shape.
- The design of the contraction is well defined nowadays and a set of given references could lead to a reasonable shape. Additional tools, such as CFD simulations, are quite welcomed to help improving the final design and/or identify some problems with the flow uniformity.
- For a medium-to-big-size wind tunnel, the choice of including a settling chamber with honeycombs is somewhat intriguing. The cost associated with aluminum honeycombs is still very high and requires special attention for providing a solution

to incorporate the panels in the cross-section area of the settling chamber. We recommend the inclusion of such device for improving the flow quality and uniformity in the test section.

- Regarding the flow analysis, a computational approach is quite indicated for this kind of design. Both 2-D and 3-D simulations could provide a good insight into how the flow is inside the tunnel, leading to additional ideas to improve the geometric shape. It is highly recommended to proceed with such simulations as soon as the first design is achieved.
- Finally, we must emphasize that the wind tunnel construction is doubtlessly a very hardworking process, which starts with the selection of the right manufacturing techniques passing by the choice of responsible workforce for building the equipment. These aspects put together will impose limitations and risks for the construction phase, which must be properly addressed by the wind tunnel designers.

This wind tunnel was built in 12 months with a specialized team of technicians who followed the original design point by point, having quality inspections every week. This wind tunnel is nowadays the main equipment of the Centro de Pesquisa em Aerodinâmica Experimental (CPAERO) in the Curso de Engenharia Aeronáutica at the Universidade Federal de Uberlândia, Minas Gerais State, Brazil. Preliminary tests indicated that the requirements of speed and flow quality have been met with success. The increase in temperature during tunnel operation due to closed-circuit energy buildup was considered satisfactory and it was kept below 5 °C for the maximum velocities tested. Some hints for designing and tips for the construction phase of similar equipment have been given in this study looking to help further initiatives into this field.

ACKNOWLEDGEMENTS

The authors would like to thank the Financiadora de Estudos e Projetos (FINEP — 0138/11) for funding this wind tunnel design and the administration of the Universidade Federal de Uberlândia (UFU) for all the support during the phases of this project. Also, the authors recognize the support of the Fundação de Amparo à Pesquisa do Estado de Minas Gerais (FAPEMIG). We also would like to recognize the effort of Prof. Aristeu da Silveira Neto (Laboratório de Mecânica de Fluidos — MFLAB), who has contributed to some design guidance and for administrative help at early stages of this project. Special thanks are given to Mr. Erick Nilson Rodrigues da Cunha (Fábrica Brasileira de Aeronaves), who worked hard and continuosly during the design and construction phase of this project. His decisions helped to improved the quality of the whole equipment.

AUTHOR'S CONTRIBUTION

Conceptualization, Almeida O; Methodology, Almeida O, Miranda FC, Ferreira Neto O and Saad FGR; Investigation, Almeida O, Miranda FC, Ferreira Neto O, and Saad FG; Writing – Original Draft, Almeida O, Miranda FC, Ferreira Neto O, and Saad FG; Writing – Review & Editing, Almeida O; Funding Acquisition, Almeida O; Resources, Almeida O; Supervision, Almeida O.

REFERENCES

Almeida O, Miranda FC, Neto OF (2016) A comparative study for propeller blade design. Therm Eng 15(2):30-37.

Barlow JB, Rae Jr WH, Pope A (1999) Low-speed wind tunnel testing. 3rd edition. New York: John Wiley and Sons.

Bell JH, Mehta RD (1988) Contraction design for small low-speed wind tunnels. CR 177488. Contract NASA-NCC-2-294. Washington: NASA.

Bell JH, Mehta RD (1989) Boundary-layer predictions for small low-speed contractions. AIAA J 27(3):372-374. doi: 10.2514/3.10122

Calautit JK, Chaudhry HN, Hughes BR, Sim LF (2014) A validated design methodology for a closed-loop subsonic wind tunnel. J Wind Eng Ind Aerodyn 125:180-194. doi: 10.1016/j.jweia.2013.12.010

Cattafesta L, Bahr C, Mathew J (2010) Fundamentals of wind-tunnel design. Hoboken: John Wiley and Sons.

Derbunivich GI, Zemskaya AS, Repik EU, Sosedko YP (1987) Effect of flow contraction on the level of turbulence. Fluid Dynam 22(2):289-294. doi: 10.1007/BF01052265

Farell C, Youssef S (1992) Experiments on turbulence management using screens and honeycombs. Project Report nº 338. Minneapolis: University of Minnesota.

Lan CE, Roskam J (1997) Airplane aerodynamics Mechanics, KTH, SE-100 and performance. Lawrence: DAR.

Lindgren B, Johansson AV (2002) Design and evaluation of a low-speed wind-tunnel with expanding corners. Technical report. Stockholm: TRITA-MEK.

Mathew J (2005) Design, fabrication and characterization of an anechoic wind tunnel facility (PhD thesis). Gainesville: University of Florida.

Mehta RD, Bradshaw P (1979) Design rules for small low speed wind tunnels. Aeronaut J 83(827):443-453. doi: 10.1017/S0001924000031985

Moonen P, Blocken B, Roels S, Carmeliet J (2006) Numerical modeling of the flow conditions in a closed-circuit low-speed wind tunnel. J Wind Eng Ind Aerodyn 94(10):699-723. doi: 10.1016/j.jweia.2006.02.001

Morel T (1975) Comprehensive design of axisymmetric wind tunnel contractions. J Fluids Eng 97(2):225-233. doi: 10.1115/1.3447255

Muncey JJ, Pote DM (1956) Design and construction of wind tunnel models. Advisory Group for Aeronautical Research and Development (AGARD-R-20). Report 20.

Pawlowski FW (1920) Théorie generale de l'helice propulsive. Paris: Gauthier-Villars.

Railway Technical Research Institute (2017) Testing facilities; [accessed 2017 July 27]. http://www.rtri.or.jp/eng/rd/testing_facilities/

Runstadler PW, Dolan FX, Dean RC (1975) Diffuser data book. Hanover: Creare, Inc.

Stratford BS (1959) The prediction of separation of the turbulent boundary layer. J Fluid Mech 5(1):1-16. doi: 10.1017/S0022112059000015

Su Y (1991) Flow analysis &and design of three-dimensional wind tunnel contractions. AIAA J 29(11):1912-1920.

Tennekes H, Lumley JL (1972) A first course in turbulence. Cambridge: MIT Press.

White FM (2003) Fluid mechanics. Boston: McGraw-Hill.